RAA 2021 Vol. **21** No. **3**, 75(8pp) doi: 10.1088/1674-4527/21/3/75

http://www.raa-journal.org *http://iopscience.iop.org/raa*

***R**esearch in*
***A**stronomy and*
***A**strophysics*

Detection of a high-confidence quasi-periodic oscillation in radio light curve of the high redshift FSRQ PKS J0805–0111

Guo-Wei Ren[1,2], Hao-Jing Zhang[1], Xiong Zhang[1], Nan Ding[3], Xing Yang[1], Fu-Ting Li[1], Pei-Lin Yan[1] and Xiao-Lin Xu[1]

[1] College of Physics and Electronics, Yunnan Normal University, Kunming 650500, China; *kmzhanghj@163.com*
[2] Department of Astronomy, Xiamen University, Xiamen 361005, China
[3] School of Physical Science and Technology, Kunming University, Kunming 650214, China

Received 2019 December 21; accepted 2020 September 20

Abstract In this work, we have searched for quasi-periodic oscillations (QPOs) in the 15 GHz light curve of the FSRQ PKS J0805–0111 monitored by the Owens Valley Radio Observatory (OVRO) 40 m telescope during the period from 2008 January 9 to 2019 May 9, using the weighted wavelet Z-transform (WWZ) and the Lomb-Scargle Periodogram (LSP) techniques. This is the first time to search for a periodic radio signal in the FSRQ PKS J0805–0111 by these two methods. Both methods consistently reveal a repeating signal with a periodicity of 3.38± 0.8 yr (>99.7% confidence level). In order to determine the significance of the periods, the false alarm probability method was applied, and a large number of Monte Carlo simulations were performed. As possible explanations, we discuss a number of scenarios including the thermal instability of thin disks scenario, the spiral jet scenario and the binary supermassive black hole scenario. We expect that the binary black hole scenario, where the QPO is caused by the precession of binary black holes, is the most likely explanation. FSRQ PKS J0805-0111 thus could be a good binary black hole candidate. In the binary black hole scenario, the distance between the primary black hole and the secondary black hole is about 1.71×10^{16} cm.

Key words: active galactic nuclei: flat spectrum radio quasar: individual: PKS J0805–0111 — galaxies: jets — method: time series analysis

1 INTRODUCTION

Active galactic nuclei (AGNs) are very energetic extragalactic sources and they are generally powered by accreting supermassive black holes (SMBHs) with masses of $10^6 - 10^{10}$ $M_\odot$ in the centers of galaxies (Gupta et al. 2019; Esposito et al. 2015). Blazars represent an extreme subclass of radio-loud AGNs with their relativistic jets aligned very closely to observers' line of sight, and they are characterized by large amplitude, rapid and violent variability across the entire electromagnetic spectrum, high and variable polarization at radio and optical energies, with non-thermal continuum emission ranging from radio to high-energy γ-rays, and superluminal jet speeds (Urry & Padovani 1995; Angel & Stockman 1980; Xiong et al. 2017). Blazars are often subclassified into two categories according to their observed features: BL Lacertae objects (BL Lac) and flat spectrum radio quasars (FSRQs). BL Lac have featureless optical spectra with weak or no emission lines, possibly due to the emission being dominated by the jet, while FSRQs have a flat radio spectrum with a spectral index $\alpha \leqslant 0.5$ and broad quasar-like emission lines in the optical spectra. The blazars' emission is dominated by relativistic jets, and the beaming effect boosts the relativistic jets (Sandrinelli et al. 2016). The blazars' broadband spectral energy distributions (SEDs) have an obvious double-peaked structure. These two peaks have different physical origins: The low-energy peak at the infrared-optical-ultraviolet band is considered to be caused by the synchrotron emission of relativistic electrons, and the high-energy peak at the GeV-TeV gamma-ray band is explained by the inverse Compton (IC) scattering (Xiong et al. 2017; Böttcher 2007; Dermer 1995).

Blazars' light curves generally display a series of features, especially aperiodic or quasi-periodic variability in a wide range of temporal frequencies. Blazars exhibiting signatures of quasi-periodic oscillations (QPOs) in the multi-frequency blazar light curves, including radio,

optical, X-ray and γ-ray, have been found (Bhatta 2018). The QPOs occur on different timescales, from decades down to a few minutes (Gupta 2018; Bhatta 2017; Bhatta et al. 2016). Research on QPOs of blazars is one of the most active fields of extragalactic astronomy, and provides an important way to explore the radiation mechanism in blazars (Li et al. 2018). According to the time spans of the variability, the characteristic timescales of variabilities can be broadly divided into three classes, viz., intraday variability (IDV) or micro-variability, which is defined as having timescales ranging from minutes to a few hours, short-term timescale variability (STV), which has timescales of days to weeks, even months, and long-term timescale variability (LTV) of a few months to years (Gupta et al. 2016; Xiong et al. 2017; Li et al. 2018). The discovery of QPO in the light curve variability could have deep consequences on the global understanding of the sources, constituting a fundamental building block of models (Sandrinelli et al. 2016). More long-term observations are needed to search for periodic variations on many timescales.

The blazar PKS J0805–0111 (RA=08h 05m 12.9s, Dec=–01d 11m 37s; and Z=1.388) was identified as an FSRQ. This source has been detected by many currently available instruments. It is cataloged by Fermi/LAT as 3FGL J0805.2–0112 (Acero et al. 2015), and its optical (R-band) brightness was recorded to be 17.87 mag (Healey et al. 2008). Since 2008, PKS J0805–0111 has been monitored in the 15 GHz radio band by the 40 m telescope of the Owens Valley Radio Observatory (OVRO) (Richards et al. 2011).

In this paper, we analyze the long term ($\sim$11.3 yr) observations of FSRQ PKS J0805–0111 and report our discovery of a high confidence QPO with 15 GHz radio flux variability. In Section 2, we describe the 15 GHz radio observations. In Section 3, we present time series analysis of the light curve using the weighted wavelet Z-transform (WWZ) and Lomb-Scargle Periodogram (LSP). We test these two methods with astronomical analog signals, moreover, we also elaborate on the false alarm probability (FAP) and the Monte Carlo (MC) simulation technique which is employed to compute the statistical significance of the detected periodicity. In Section 4, we discuss three scenarios to explain the QPO behavior of FSRQ PKS J0805–0111, and estimate the distance between the primary black hole and the secondary black hole. Our conclusions are summarized in Section 5.

2 OBSERVATIONS

OVRO announced 15 GHz radio band observation data from the source FSRQ PKS J0805–0111, observed with a 40-meter telescope from 2008 January 9 to 2019 May 9 for a total of 4138 d ($\sim$11.3 yr) and a total of 507 data points. We conducted a preliminary analysis of these data. In the 15 GHz radio band data of this source, the minimum flux is 0.14 Jy, the maximum flux is 0.76 Jy, the average flux is 0.44 Jy and the standard deviation is 0.14. In order to quantify the observed variability, we estimate the variability amplitude (VA), which represents the peak-to-peak oscillation, and the fractional variability (FV), which corresponds to the mean variability. We estimate the amplitude of peak-to-peak variation utilizing the relationship given in Heidt & Wagner (1996)

$$VA = \sqrt{(A_{\rm max} - A_{\rm min})^2 - 2\sigma^2}\,, \tag{1}$$

where $A_{\rm max}$, $A_{\rm min}$ and σ represent the maximum value, minimum value and average value of the magnitude errors in the radio observation data, respectively. Similarly, we can calculate the FV with a mean flux of $\langle F \rangle$ with S^2 variance, and $\langle \sigma_{\rm err}^2 \rangle$ is the mean squared error, as stated in the formula reported in Vaughan et al. (2003)

$$F_{\rm var} = \sqrt{\frac{S^2 - \langle \sigma_{\rm err}^2 \rangle}{\langle F \rangle^2}}\,. \tag{2}$$

The error of FV can be estimated by relying on the formula given in Aleksić et al. (2015)

$$\sigma_{F_{\rm var}} = \sqrt{{F_{\rm var}}^2 + \sqrt{\frac{2}{N}\frac{\langle {e_{\rm err}}^2 \rangle^2}{\langle F \rangle^4} + \frac{4}{N}\frac{\langle {\sigma_{\rm err}}^2 \rangle}{\langle F \rangle^2}{F_{\rm var}}^2}} - F_{\rm var}\,. \tag{3}$$

In this case, we can get $VA = 0.62$ and $F_{\rm var} = 0.31 \pm 0.03$ through the above expression, which shows that there is a modest change in this source during this time. Figure 1 displays the light curve of PKS J0805–0111, and the blue curve is a sinusoidal fitting curve, which is plotted to help indicate modulation in the light curve. As can be seen from Figure 1, there is a clear outbreak of activity in this source, and four distinct peaks can be clearly discerned. From the light curve, we can visually see that this source has a QPO between 1100 d and 1300 d.

3 LIGHT CURVE ANALYSIS AND RESULTS

The 15 GHz radio band light curve of FSRQ PKS J0805–0111, for observations taken from 2008 January 9 to 2019 May 9, is plotted in Figure 1. A visual inspection indicates a possible QPO in the observations made during the whole observation period.

We carried out QPO search analysis using two methods of long time-series analysis: WWZ and LSP. We discuss the methods, analysis and results in detail below.

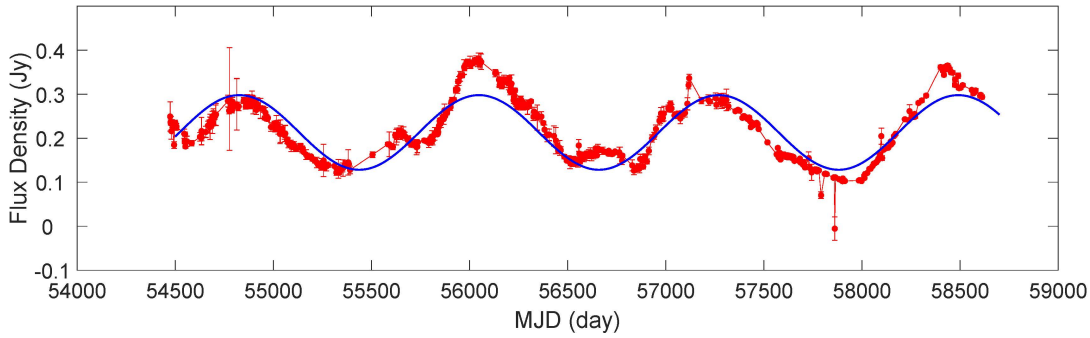

Fig. 1 Long-term light curve of FSRQ PKS J0805–0111 at 15 GHz on 2008 January 9 to 2019 May 9 (MJD 54474 to 58612) obtained from OVRO. The data integration time is 4138 d (∼11.3 yr). The *blue sinusoidal curve* (with a period of 3.38 yr) is plotted to help indicate the modulation in the light curve.

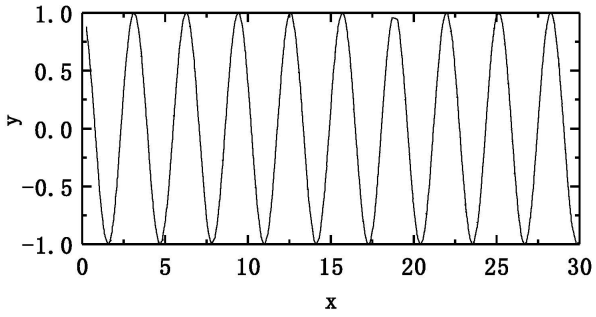

Fig. 2 Graph of cosine function representing analog periodic signals.

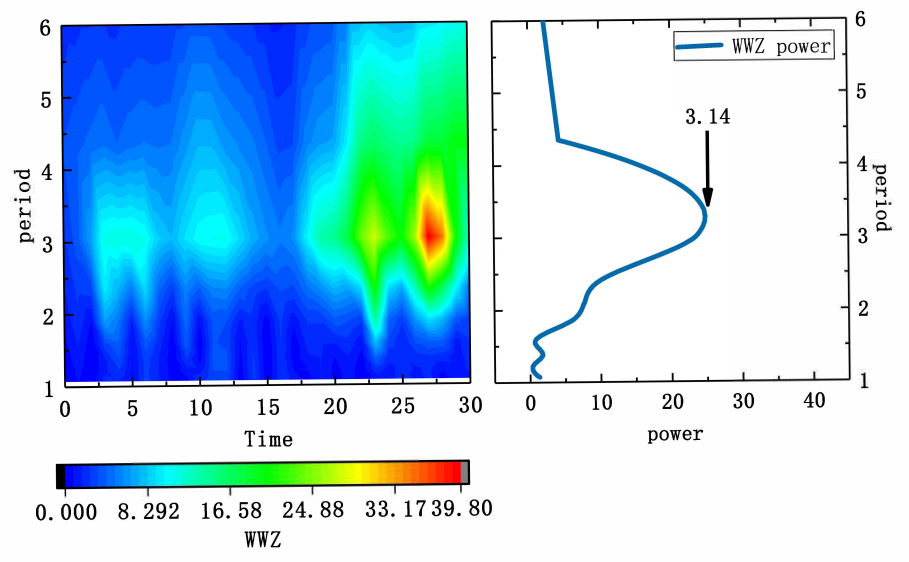

Fig. 3 Periodic analysis of the cosine function by the WWZ transform.

3.1 Astronomical Analog Signal Test

In order to test the reliability of the WWZ and LSP methods, we utilized an analog periodic signal to compare with the astronomical observation data for verification. In this paper, we tested the accuracy of the two research methods by the cosine function $y = \cos 2\pi$ with a period of π as illustrated in Figure 2. The test results of these two methods are explained as follows: Figure 3 features the periodic analysis results of the cosine function by the WWZ method, and the periodic analysis results of the sinusoidal function by the LSP method are depicted in Figure 4.

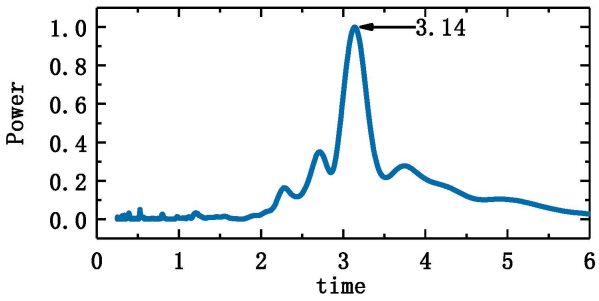

Fig. 4 Periodic analysis of the cosine function by the LSP method.

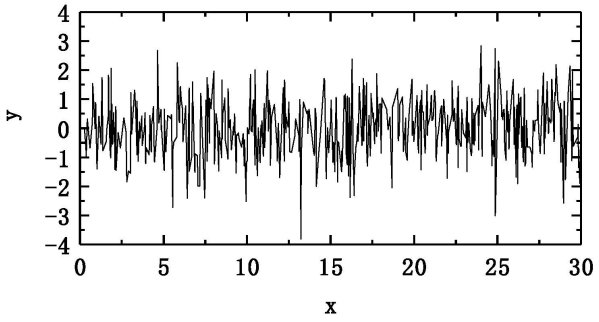

Fig. 5 Random noise.

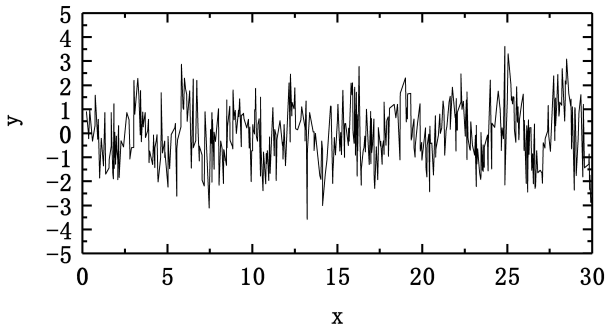

Fig. 6 Superimposed graph of random noise and cosine function.

In order to further determine the reliability of the WWZ and LSP methods in analyzing observations, we added random noise data to the periodic signal data of the cosine function simulation, and these two methods were tested again. The specific process was calculated by a Python program, and the test results are as follows: Figure 5 shows random noise, and the superimposed graph of random noise and cosine function is plotted in Figure 6. Figures 7 and 8 display the results of periodic analysis for the cosine function, with random noise added, by the WWZ and LSP methods, respectively.

The results confirm that the standard cosine simulation data and the cosine simulation data with random noise were analyzed successfully by the WWZ and LSP methods, which is the same as $T \approx 3.14$. This demonstrates that applying these two methods for periodic research is reliable.

3.2 Weighted Wavelet Z-transform

Wavelet analysis simultaneously decomposes data into time and frequency domains to estimate and determine the significance of a period (Gupta et al. 2019). However, we utilized wavelet analysis to process non-equal interval data in practice, and interpolation was used to reduce the impact of astronomical observation signals that are affected by the observation season, the weather and the phase of the Moon, but this has a great influence on the authenticity of the data.

We calculated the WWZ power for a given time and frequency by the WWZ method (King et al. 2013; Bhatta et al. 2016; Bhatta 2017; Gupta et al. 2019). It is defined by Foster (1996), who points out that the analysis result can be significantly improved, and the period can be obtained more accurately, if the wavelet transform is regarded as the projection of the vector.

3.3 Lomb-Scargle Periodogram

LSP (Foster 1996) is widely utilized to determine if QPOs are present in the observations. It is a popular method of time series analysis (Bhatta et al. 2016; Bhatta 2017, 2018). The method is a discrete Fourier transform (DFT)-based periodic extraction algorithm. The LSP's basic principle is fitting a series of trigonometric functions by the least-squares method via a linear combination in the form $y = a\cos\omega t + b\sin\omega t$, and thus the characteristics of a signal are converted from the time domain to the frequency domain (Scargle 1982). For a non-uniformly sampled time series $x(t_i)$, $i = 1, 2, 3 \cdots, N$, the power spectrum is defined as

$$P_{\mathrm{LS}}(f) = \frac{1}{2N} \times \left[\frac{\left\{ \sum_{i=1}^{N} x(t_i) \cos\left[2\pi f (t_i - \tau)\right] \right\}^2}{\sum_{i=1}^{N} \cos^2\left[2\pi f (t_i - \tau)\right]} + \frac{\left\{ \sum_{i=1}^{N} x(t_i) \sin\left[2\pi f (t_i - \tau)\right] \right\}^2}{\sum_{i=1}^{N} \sin^2\left[2\pi f (t_i - \tau)\right]} \right]^2 . \quad (4)$$

The parameters f and τ represent the test and time offset, respectively, which can be obtained by the following formula,

$$\tan(2\pi f\tau) = \frac{\sum_{i=1}^{N} \sin 2\pi f t_i}{\sum_{i=1}^{N} \cos 2\pi f t_i} . \quad (5)$$

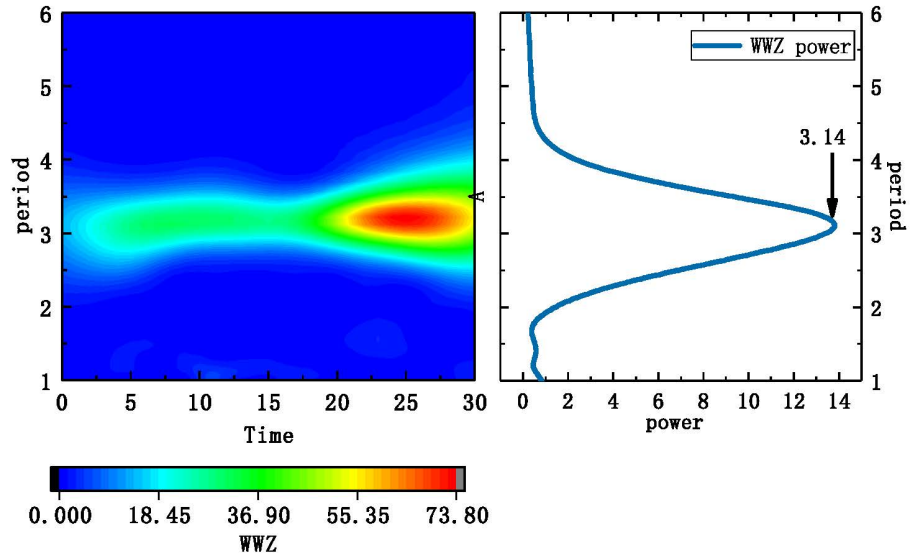

Fig. 7 Periodic analysis of the random noise and sinusoidal function by the WWZ method.

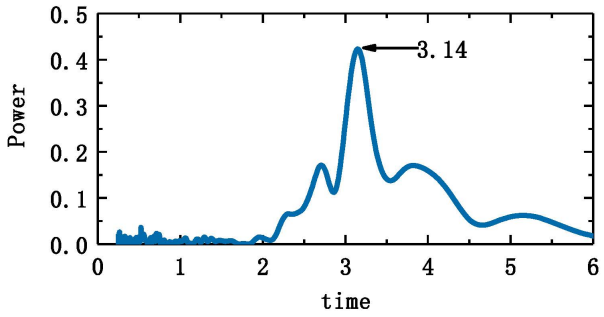

Fig. 8 Periodic analysis of the random noise and sinusoidal function by the LSP method.

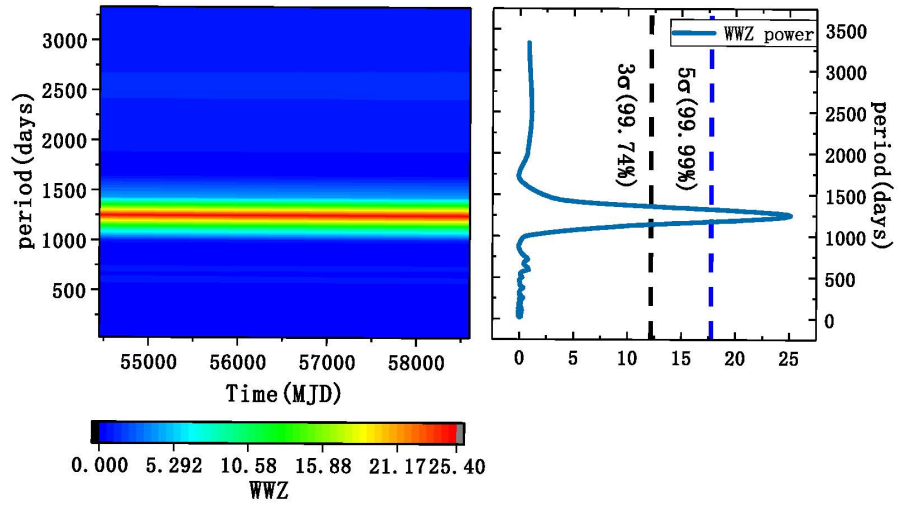

Fig. 9 WWZ of the light curve presented in Fig. 9. The *left panel* displays the distribution of color-scaled WWZ power (with red most intense and blue lowest) in the time-period plane; the *right panel* features the time-averaged WWZ power (*solid blue curve*) as a function of period showing that a distinct peak stands out around the timescale of 1250 ± 214 d; the *black dashed line* indicates the threshold of FAP fixed at 3σ (99.74%), and the *blue dashed line* signifies the threshold of FAP fixed at 5σ (99.99%).

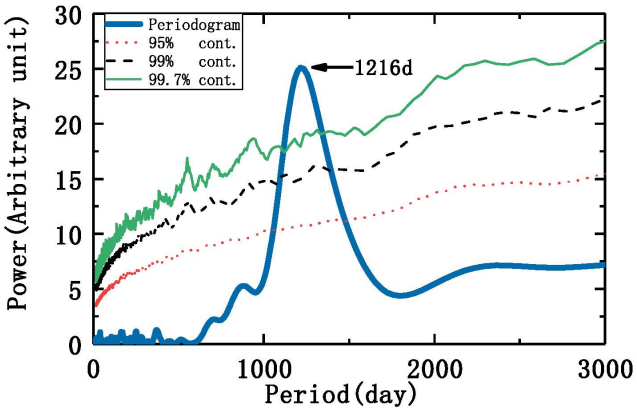

Fig. 10 The results of the LSP analysis for the period search, showing a distinct peak which stands out around the timescale of 1216 ± 373 d. The *red*, *black* and *green curves* represent the 95%, 99% and 99.7% significance levels, respectively, from MC simulations.

3.4 The Variability Analysis and Results of FSRQ PKS J0805-0111

In this paper, we analyze the 15 GHz radio observations of the source FSRQ PKS J0805–0111, announced by OVRO, applying the WWZ and LSP methods. We ascertain that the QPO of this source is about 3.38 yr.

In order to search for QPOs of the source FSRQ PKS J0805–0111, we analyzed the 15 GHz flux density variations by the WWZ method at first, which is one of the most common time series analysis methods. The WWZ transform of the FSRQ PKS J0805–0111 light curve was computed for the minimum and maximum frequencies of $f_{\min} = 1/4138$ and $f_{\max} = 1/25$, respectively. The results are shown in Figure 9. The most significant spectral power peak is yielded by WWZ, and we further estimate its significance level by testing the FAP of the null hypothesis. The probability that $P_N(\omega) = P_{\rm LS}(\omega)/\sigma^2$ will be between some positive z and $z + dz$ is e^{-z}. If we scan some N_i independent frequencies, the probability that none give values larger than z is $(1 - e^{-z})^{N_i}$: $p(> z) \equiv 1 - (1 - e^{-z})^{N_i}$, which is FAP (Ciaramella et al. 2004); The smaller the FAP, the higher degree is the significance for the peak.

We analyzed the ∼11.3 yr long OVRO light curve of FSRQ PKS J0805–0111, and the results are as follows: It manifests a distinct peak around the timescale of 1250 ± 214 d with a single-trial FAP significance of 5.75×10^{-8}, which represents a very strong periodicity in the associated periodic signal. We estimated the period uncertainty by calculating the 3σ (99.74%) and 5σ (99.99%) confidence intervals on the observed period, by the FAP method.

We performed the LSP analysis of the entire light curve in order to further confirm the presence of the above QPO by the different method.

We applied the LSP method to the observations. The LSP method of the FSRQ PKS J0805+0111 light curve was computed for the minimum and maximum frequencies of $f_{\min} = 1/4138$ and $f_{\max} = 1/25$, respectively. What needs to be emphasized is that the estimate of the total number of periodogram frequencies n_0 is critical to the evaluation of the periodogram. In this work, we evaluate the total number of periodogram frequencies by relying on

$$N_{\rm eval} = n_0 T f_{\max}\,. \tag{6}$$

Since the observations we get are not equally spaced, spurious peaks may be generated, which make it difficult to estimate the confidence of the peak height in the power spectrum. So, we should consider this effect in this case. The red noise process may be the product of periodic variability in blazars, and the red noise was modeled as an approximate power law power spectral density (PSD): $P \propto f^{-\alpha} + C$. We modeled the wavelength variability as red noise with a power law index α to assess the confidence of our findings. We then performed an MC simulation technique (Timmer & Koenig 1995) for determining the significance of the periods, and a large number of (typically 20 000) light curves were simulated for every spectral slope α value. We obtained the α index by fitting the spectrum of the periodogram with a power law. Using an even sampling interval to simulate 10 000 light curves, we computed their LSP. Figure 10 depicts the results, showing a distinct peak that stands out around the timescale of 1216 ± 373 d. The local 95%, 99% and 99.7% MC simulation contours are represented by the red, black and the green curves, respectively.

4 DISCUSSION

Generally, some periodic or quasi-periodic behaviors were displayed in the light curves of blazars. Studying these periodic or quasi-periodic behaviors is an important method

to investigate the nature of the physical mechanisms within the emission regions. However, many researchers have reported the QPOs of a few blazars at different wavelengths on diverse timescales. They can be approximately divided into three classes, viz., IDV, STV and LTV. Studies on QPOs could provide novel insights into a number of blazar aspects, and some physical models have been reported by many researchers, e.g., a binary SMBH AGN system (Lehto & Valtonen 1996; Valtaoja et al. 2000; Fan et al. 2007), helical structure in inner jets (Conway & Murphy 1993), precessing accretion disk model (Katz 1997) and the thermal instability of thin disks scenario. The observed periodic flux modulations could be explained by a number of models.

In this paper, we have attempted to detect the possible periodicity of the FSRQ PKS J0805–0111 in the radio 15 GHz light curve using the OVRO observations acquired during the period from 2008 January 9 to 2019 May 9 (MJD 54474 to 58612). The period of the 15 GHz radio band is 1250 ± 214 d by WWZ analysis; the confidence interval on the observed period is more than $5\sigma(99.99\%)$, by the FAP method; the period of 15 GHz radio band by LSP analysis is 1216 ± 373 d and the significance level is more than 99.7%, from MC simulations. It can be concluded that the QPO of FSRQ PKS J0805–0111 is 3.38 ± 0.8 yr ($> 99.7\%$ confidence level).

Although the physical mechanism in blazars on long-term timescales is not well understood, some possible interpretations, such as (1) the thermal instability of thin disks scenario; (2) the spiral jet scenario; (3) the binary SMBH scenario, have been applied to explain long-term periodic variability. In the scenario of thermal instability of thin disks, the cyclic periodic outburst is lead by thermal instability of a thin disk. The uncertainty of the disk causes the related outburst of the jet because there is a certain degree of link between jet and disk. Random light variations could be produced by thermal instability of thin disks in jets with stochastic red noise characteristics, and this process is stochastic (Li et al. 2017). Hence, this scenario could be responsible for long-term QPO.

In the spiral jet scenario, the relativistic beaming effect leads to QPO behavior of blazars. The change in relativistic beaming effect causes obvious flux variations to arise because the different parts of such a helical jet pass closest to the line of sight, even though the emission from the jet has no intrinsic variations. Furthermore, the viewing angle to the helical motion changes periodically when the emission blob of the jet moves toward us, thereby resulting in QPOs (Zhou et al. 2018). However, it needs to be noted that low-frequency radio emission such as 15 GHz is less affected by the beaming effect, due to it generally being considered to be dominated by the extended jet structure of the jet (Fan & Wu 2018).

Consequently, we are investigating if the QPO behavior in the FSRQ PKS J0805–0111 may be caused by the binary SMBH model, which possibly can explain the presence of year-like LTV in AGNs (Komossa 2006). An SMBH system would lead to a wiggling or precessing jet because of the orbital motion or rotation, i.e., there is a precession motion of a relativistic jet in an orbit due to the gravitational torque induced by the non-coplanar secondary black hole in the primary accretion disk, which produces the observed LTVs ranging from a few to tens of years (Katz 1997; Caproni et al. 2013).

If we assume that the long-term light variations of blazars are caused by the binary SMBH model, then the distance between the primary black hole and the secondary black hole can be calculated. For the binary black hole mass ratio, Qian et al. (2007) discussed the secondary black hole and primary black hole ratio being about 1, and Caproni & Abraham (2004) think this ratio is about 0.78. In this case, we calculated that the average of these two values is 0.89, and we use this value as the ratio of the secondary black hole mass and the primary black hole mass. In addition, we obtain 293 black hole masses of typical blazars (Shen et al. 2011; Shaw et al. 2012; Liu et al. 2006; Wang et al. 2004; Chai et al. 2012; Sbarrato et al. 2012; Zhou & Cao 2009; Zhang et al. 2012; Xie et al. 1991, 2004), and we calculate that the average value of these blazars' black hole mass is $\bar{M} = 10^{8.6}\,M_{\odot}$. We assume that this is the primary black hole mass, and we take a binary black hole mass ratio of 0.89, therefore, the secondary black hole mass can be calculated as $m = 0.89\bar{M} = 0.89 \times 10^{8.6}\,M_{\odot}$. The relevant parameters of the binary black hole model according to the orbital period can calculated.

In this case, we take $P_{\rm obs} = 3.38$ yr, $M = 10^{8.6}\,M_{\odot}$ and $m = 0.89 \times 10^{8.6}\,M_{\odot}$, according to Kepler's third law

$$\left(\frac{P_{\rm obs}}{1+z}\right)^2 = \frac{4\pi^2 a^3}{G\,(M+m)}\,, \tag{7}$$

where Z, a and G represent the redshift, the distance between the primary black hole and the secondary black hole, and universal gravitational constant respectively, thus we can calculate that the distance between the primary black hole and the secondary black hole is $a \sim 1.71 \times 10^{16}$ cm.

5 CONCLUSIONS

In this paper, we have searched for QPOs in the 15 GHz light curve of the FSRQ PKS J0805–0111 monitored by the OVRO 40 m telescope during the period from 2008 January 9 to May 9. Our main results are as follows:

(1) We have found a quasi-periodic signal with a period of 3.38 ± 0.8 yr ($> 99.7\%$ confidence level) in the 15 GHz radio light curve of the FSRQ PKS J0805–0111 by the WWZ and LSP methods. This is the first time that a quasi-periodic signal has been detected in this source.

(2) In the scenario where the precession of binary SMBHs causes radio quasi-periodic variability, the distance between the primary black hole and the secondary black hole is about 1.71×10^{16} cm.

This source could be a good binary SMBH candidate. We will further monitor the optical variability of the source in the optical band to further verify whether there is precession of binary SMBHs.

Acknowledgements This work is supported by the National Natural Science Foundation of China (Grant No. 11663009), and the High-Energy Astrophysics Science and Technology Innovation Team of Yunnan Higher School.

This research has made use of data from the OVRO 40-m monitoring program (Fan & Wu 2018) which is supported in part by NASA grants NNX08AW31G, NNX11A043G and NNX14AQ89G, and NSF grants AST-0808050 and AST-1109911.

References

Acero, F., Ackermann, M., Ajello, M., et al. 2015, ApJS, 218, 23
Aleksić, J., Ansoldi, S., Antonelli, L. A., et al. 2015, A&A, 576, A126
Angel, J. R. P., & Stockman, H. S. 1980, ARAA, 18, 321
Bhatta, G., Zola, S., Stawarz, Ł., et al. 2016, ApJ, 832, 47
Bhatta, G. 2017, ApJ, 847, 7
Bhatta, G. 2018, Galaxies, 6, 136
Böttcher, M. 2007, APSS, 309, 95
Caproni, A. & Abraham, Z. 2004, ApJ, 602, 625
Caproni, A., Abraham, Z., & Monteiro, H. 2013, MNRAS, 428, 280
Chai, B., Cao, X., & Gu, M. 2012, ApJ, 759, 114
Ciaramella, A., Bongardo, C., Aller, H. D., et al. 2004, A&A, 419, 485
Conway, J. E., & Murphy, D. W. 1993, apj, 411, 89
Dermer, C. D. 1995, ApJL, 446, L63
Esposito, V., Walter, R., Jean, P., et al. 2015, A&A, 576, A122
Fan, J. H., Liu, Y., Yuan, Y. H., et al. 2007, A&A, 462, 547
Fan, X.-L., & Wu, Q. 2018, ApJ, 869, 133
Foster, G. 1996, AJ, 112, 1709
Gupta, A. C., Agarwal, A., Bhagwan, J., et al. 2016, MNRAS, 458, 1127
Gupta, A. 2018, Galaxies, 6, 1
Gupta, A. C., Tripathi, A., Wiita, P. J., et al. 2019, MNRAS, 484, 5785
Healey, S. E., Romani, R. W., Cotter, G., et al. 2008, ApJS, 175, 97
Heidt, J., & Wagner, S. J. 1996, A&A, 305, 42
Katz, J. I. 1997, apj, 478, 527
King, O. G., Hovatta, T., Max-Moerbeck, W., et al. 2013, MNRAS, 436, L114
Komossa, S. 2006, memsai, 77, 733
Lehto, H. J., & Valtonen, M. J. 1996, ApJ, 460, 207
Li, X.-P., Luo, Y.-H., Yang, H.-Y., et al., 2017, ApJ, 847, 8
Li, X.-P., Luo, Y.-H., Yang, H.-Y., et al. 2018, ApSS, 363, 169
Liu, Y., Jiang, D. R., & Gu, M. F. 2006, ApJ, 637, 669
Qian, S.-J., Kudryavtseva, N. A., Britzen, S., et al. 2007, ChJAA (Chin. J. Astron. Astrophys.), 7, 364
Richards, J. L., Max-Moerbeck, W., Pavlidou, V., et al. 2011, ApJS, 194, 29
Sandrinelli, A., Covino, S., Dotti, M., & Treves, A. 2016, AJ, 151, 54
Sbarrato, T., Ghisellini, G., Maraschi, L., & Colpi, M. 2012, MNRAS, 421, 1764
Scargle, J. D. 1982, ApJ, 263, 835
Shaw, M. S., Romani, R. W., Cotter, G., et al. 2012, ApJ, 748, 49
Shen, Y., Richards, G. T., Strauss, M. A., et al. 2011, ApJS, 194, 45
Timmer, J., & Koenig, M. 1995, A&A, 300, 707
Urry, C. M., & Padovani, P. 1995, PASP, 107, 803
Valtaoja, E., Teräsranta, H., Tornikoski, M., et al. 2000, ApJ, 531, 744
Vaughan, S., Edelson, R., Warwick, R. S., & Uttley, P. 2003, MNRAS, 345, 1271
Wang, J.-M., Luo, B., & Ho, L. C. 2004, ApJ, 615, L9
Xie, G. Z., Liu, F. K., Liu, B. F., et al. 1991, A&A, 249, 65
Xie, G. Z., Zhou, S. B., & Liang, E. W. 2004, AJ, 127, 53
Xiong, D., Bai, J., Zhang, H., et al. 2017, ApJS, 229, 21
Zhang, J., Liang, E.-W., Zhang, S.-N., & Bai, J. M. 2012, ApJ, 752, 157
Zhou, M., & Cao, X.-W. 2009, RAA, 9, 293
Zhou, J., Wang, Z., Chen, L., et al. 2018, Nature Communications, 9, 4599